New Physics: Sae Mulli,
Vol. 67, No. 6, June 2017, pp. 684∼695
http://dx.doi.org/10.3938/NPSM.67.684

Tunable Optical Responses of a Graphene-Gold Nanoparticle Composite for Visible Light

Sangmo CHEON
Department of Physics, Hanyang University, Seoul 04763, Korea

Chang-Won LEE*
School of Basic Sciences, Hanbat National University, Daejeon 34158, Korea

Chan-Wook BAIK
Samsung Advanced Institute of Technology, Suwon 16678, Korea

Heejeong JEONG†
Department of Physics and Institute for Advanced Study,
The Hong Kong University of Science and Technology, Clear Water Bay, Hong Kong

(Received 31 January 2017 : revised 22 February 2017 : accepted 24 February 2017)

Applying Maxwell-Garnett's effective medium model, we theoretically study the optical properties of graphene with gold nanoparticles as a function of the particle volume fraction, size of the particles, chemical potential, and temperature. To account for the visible spectrum at energies less than 3 eV, we consider up to the second order of the optical conductivity calculated using the tight-binding model. Randomly distributed gold nanoparticles have a strong influence on the optical responses of graphene, such as its absorption, reflection, and transmission, thus allowing enhanced optoelectronic properties. We find that the composite can be made to serve as a potential tunable photonic material for a reflective optical modulator by controlling the local plasmonic resonance of the nanoparticle, volume fraction, and chemical potential.

PACS numbers: 76.87.Wj
Keywords: Graphene, Metal nanoparticles, Optical conductivity

I. INTRODUCTION

Graphene is an atomically thin material which is made only of carbon atoms arranged in a hexagonal lattice [1]. It has been attracting much attention as a candidate for future electronic material because of high carrier mobility, high optical transparency and exceptional mechanical flexibility and strength [2–7]. In addition, wideband absorption [8] and high carrier mobility [9] allows graphene to be considered as a new material for wideband and ultrafast photodetectors [10,11]. Recent studies have demonstrated highly enhanced multi-color graphene photodetectors by coupling graphene devices with plasmonic structures [12,13].

From electronic point of view, metal nanoparticles over graphene sheet can supply carriers to the graphene and can change Fermi level (*i.e.* chemical potential) [14]. The carrier type depends on the metal types and distances. At the same time, the metal nanoparticles have strong local surface plasmon polaritons, which significantly alters optical properties and local density of states. Even though the optical effect of the metal nanoparticles on graphene has been widely studied experimentally [14–18], it is surprisingly rare to find comprehensive theoretical studies for optical responses of the composites with respect to particle volume fraction, the size of the par-

*E-mail: cwlee42@hanbat.ac.kr
†E-mail: hjjeong@ust.hk

ticles, chemical potential, and temperature. In this article, we theoretically investigated optical properties of the composite of a graphene sheet with gold nanoparticles, by applying the Maxwell-Garnett theory. This paper is organized as follows. First, we briefly review the optical conductivity of the suspended graphene and the size-effect of the gold nanoparticles as a two-dimensional effective medium. Then we get the total conductivity of the graphene with gold nanoparticles. Third, we show normal incidence absorptance, reflectance, and transmittance spectra of the system consisting of air, nanoparticles, graphene and glass substrate under several different conditions: particle volume fraction, size of the particles, and chemical potential. We will discuss the temperature effect and the validity of the effective medium theory.

II. BRIEF REVIEW ON THE OPTICAL PROPERTIES OF THE SUSPENDED PURE GRAPHENE

Tight-binding model is a good theoretical basis to explain low energy optical properties of the intrinsic graphene [19–23]. For excitation and relaxation less than 1 eV, Dirac-cone approximation successfully explains a number of optical phenomena. For more than 1 eV, though, considering the leading order term only is not sufficient. In our calculation, we included the second order term of the tight-binding model to account for the visible range of spectrum. For higher energy E > 3.1 eV, the optical conductivity enhances owing to the increased electronic joint density of states toward van Hove singularity owing to strong carrier-carrier interaction [19]. Therefore, we restrict ourselves to the visible spectra (1.2 eV < E < 3.1 eV).

In the limit of $T/\mu \to 0$, the optical conductivity is given by intraband and interband contributions [22]:

$$\sigma = \sigma_{\text{intraband}} + \sigma_{\text{interband}}$$

$$\sigma_{\text{intraband}} = i\sigma_0 \frac{4\mu}{\pi\hbar(\omega + i\gamma)}, \quad (1)$$

$$\sigma_{\text{interband}} = \sigma_0\{\theta(\hbar\omega - |2\mu|)\} + \frac{i}{\pi}\log\left|\frac{\hbar\omega + |2\mu|}{\hbar\omega - |2\mu|}\right|, \quad (2)$$

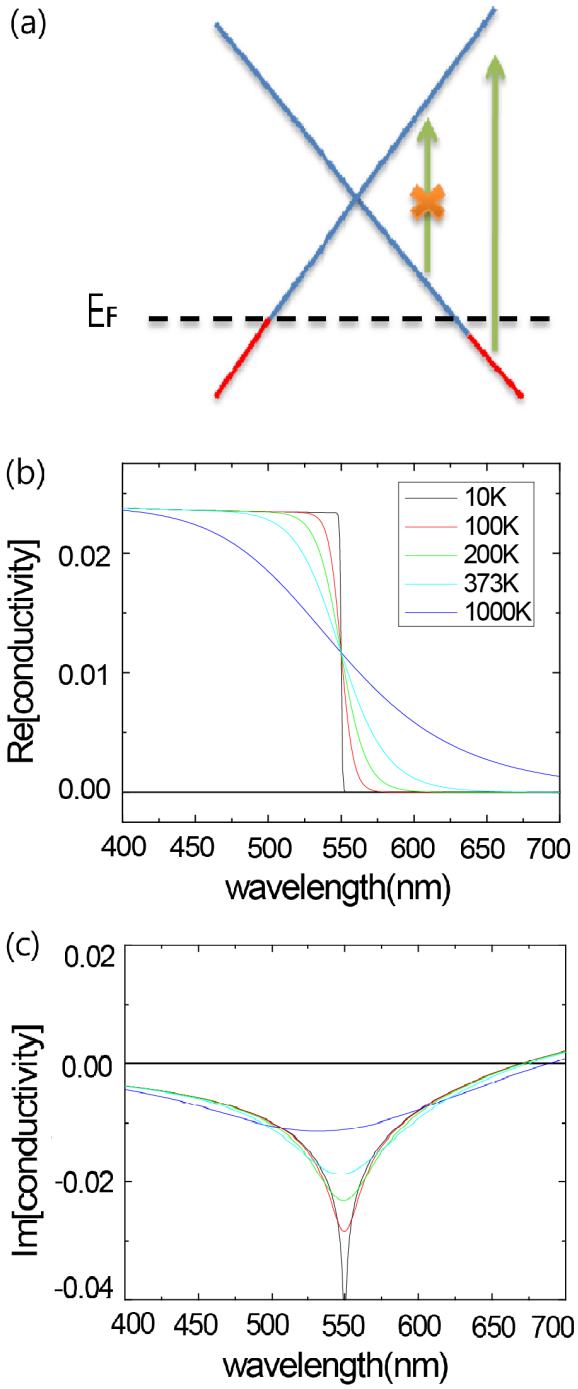

Fig. 1. (Color online) (a) In the Dirac cone of graphene, states are filled (red line) below Ef and empty (blue line) above E_f. Electronic transitions smaller than $2E_f$ are not allowed owing to Pauli blocking. Real (b) and imaginary (c) part of the optical conductivities of the suspended pristine graphene are drawn according to Eq. (3) and (4) as a function of electronic temperature.

where $\sigma_0 = e^2/4\hbar$ is termed the ac universal conductivity of the graphene. (e is the charge of an electron, $\hbar$ is

Plank constant.) The Eq. (1) shows Drude-like formula responsible for interband processes. We will set $\gamma = 0$ under an assumption that the collision rate of carriers is less than the frequency, $\gamma \ll \omega$. The $\theta(x)$ in Eq. (2) is Heaviside-step function, which determines the energy for Pauli blocking, which means the optical interband transition can only occur for frequencies larger than twice the Fermi energy, as shown in Fig. 1(a). The Eq. (1) and (2) are effectively valid for zero temperature and infrared region of the optical spectrum.

We need corrections to employ the temperature dependence in order to account for temperature increase under irradiation [23]. Then real and imaginary parts of the optical conductivity become,

$$\mathrm{Re}[\sigma] = \sigma_0 \frac{\pi}{12\sqrt{3}} \frac{t^2}{\hbar\omega} \rho(\frac{\hbar\omega}{2}) \left(18 - \left(\frac{\hbar\omega}{t}\right)^2\right) \times \left[\tanh\frac{\hbar\omega + 2\mu}{4k_gT} + \mathrm{ranh}\frac{\hbar\omega - 2\mu}{4k_gT}\right], \tag{3}$$

$$\mathrm{Im}[\sigma] \approx \sigma_0 \frac{\pi}{3\sqrt{3}} \frac{t^2}{\hbar\omega} \mathrm{Re}\left[\int_0^{3t} dE\rho(E) f\left(\frac{E}{t}\right) [f_{FD}(-E) - f_{FD}(E)] \frac{4E}{(\hbar\omega + i0^+)^2 - (2E)^2}\right], \tag{4}$$

where k_B is the Boltzmann constant, t is the hopping parameter connecting first-nearest neighbors with value of the order 3 eV, $\rho(E)$ is the density of states per spin per unit cell, $f_{FD}(x) = 1/(e^{(x-\mu)/k_BT} + 1)$ is the Fermi-Dirac function and T is the electron temperature, respectively. Here the unknown function is defined as $f(x) = 18 - 4x^2$. As temperature increases, the Heavisi de-step function used in the optical conductivity (originated from the interband transition) becomes smeared out at finite-temperature at $\hbar\omega = 2\mu$ in Eq. (2), as shown in Fig. 1(b) and (c).

III. EFFECTIVE MEDIUM APPROACH FOR GRAPHENE AND GOLD NANOPARTICLE SYSTEM

In this section, we derive the conductivity of the graphene with gold nanoparticles by applying the Maxwell-Garnett effective medium approach. We assume the hybrid system is composed of air, nanoparticles with radius R $\approx$ 10 nm, and pristine graphene, as shown in Fig. 2(a) and (b).

Unlike gold bulk, the gold nanoparticle has size-dependent optical properties owing to the quantum and classical size effects [24]. It is known that the quantum size effect is negligible for R > 2 nm [24]. Therefore, we only consider the classical size effect via the size-dependent scattering in the Drude-Lorentz model, which agrees well with the previously reported experimental data [25–27]. When the size of the gold nanoparticle is smaller than the mean free path, the size-dependent scattering at the boundary gives a contribution to the dielectric functions of a gold nanoparticle. (Note that the mean free path of gold in the Drude-Lorentz model is approximately $v_F/\gamma_0 \approx 39.2$ nm at 373 K. Here, $\gamma_0 \approx 3.57 \times 10^{13}\mathrm{s}^{-1}$ is the bulk collision frequency, $v_F \approx 1.4 \times 10^6$ m/s is the Fermi velocity of the gold.) Then the size-dependent dielectric function of gold nanoparticle is given by the follow equation.

$$\varepsilon_{\mathrm{nanoparticle}}(R,\omega) = \varepsilon_{\mathrm{exp}}(\omega) + \frac{\omega_p^2}{\omega^2 + i\omega\gamma_0} - \frac{\omega_p^2}{\omega^2 + i\omega\Gamma} \tag{5}$$

where $\varepsilon_{\mathrm{exp}}(\omega)$ is the experimental dielectric function [30], and $\omega_p \approx 1.3 \times 10^{16}(Hz)$ is the bulk plasmon frequency of gold [28]. (Here, the $\Gamma = \gamma_0 + A \times v_F/a$ is modified collision frequency by the size-dependent scattering, where a is the reduced electron mean free path and A is the geometry-dependent parameter. Here, $a = 2R$ and $A = 1$.)

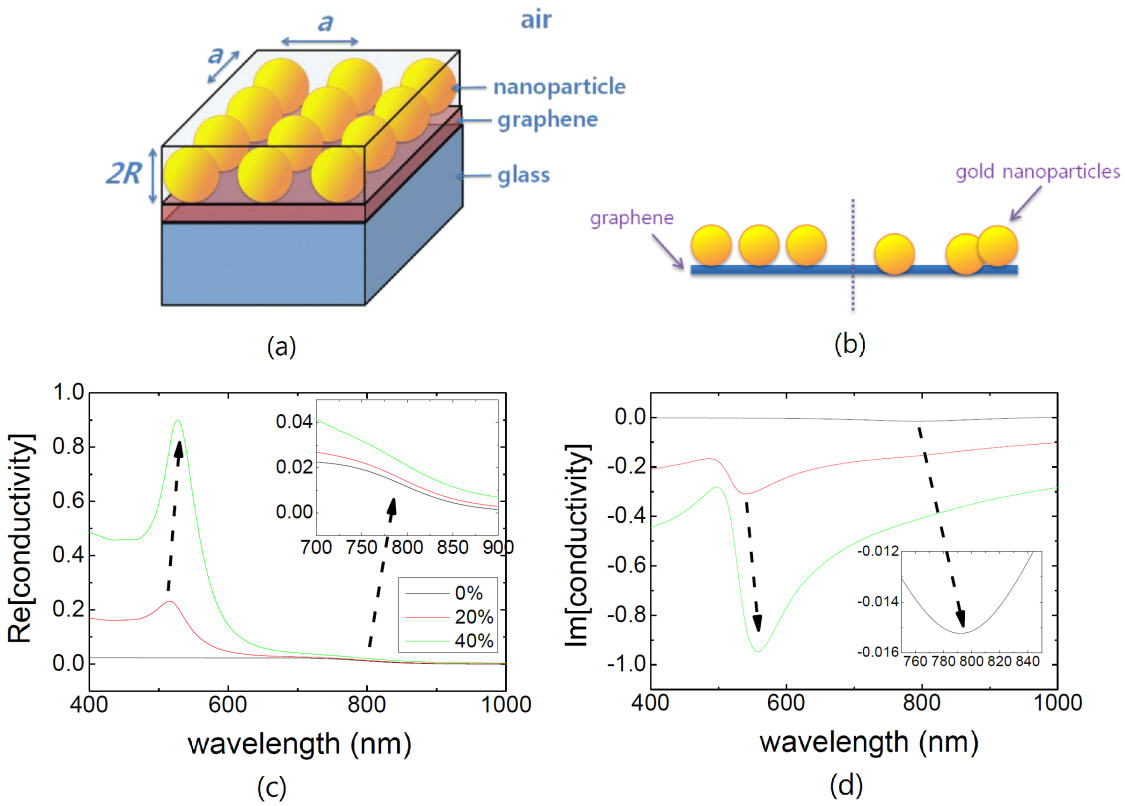

Fig. 2. (Color online) (a) The hybrid system is composed of air, nanoparticles, graphene, and a glass substrate. The radii of the nanoparticles are assumed to be in the order of 10 nm. For smaller than 2 nm radii, quantum size effect should be considered. (b) We assume the gold nanoparticles are well ordered, compatible with the assumptions of Maxwell-Garnett effective medium theory (Left). If the gold nanoparticles are sunk or overlapped, the validity of our assumption fails (Right). Real (c) and imaginary (d) part of the conductivity spectra in the visible region as a function of volume fraction of the composite; 0% (black), 20% (red), and 40% (green), respectively. The temperature is at 373 K and the chemical potential is 0.775 eV. The radius of the particle is 10 nm. With increasing volume fraction, the real part of the conductivity increases and the peak shifts to red. The inset in (c) shows the smeared Heaviside-step functions near 800 nm. The imaginary part of the conductivity decreases and the peak point is also red-shifted as the volume fraction increases. The inset in (d) shows the smeared feature near 800 nm, which was originally observed from the pure graphene as a singular point.

In carrying out calculation, three more assumptions are made. First, the single-particle scattering approach based on Mie scattering is neglected since the interparticle spacing which is the order of 100 nm is significantly smaller than the wavelength considered (400 $\sim$ 1000 nm). Second, we neglect the effect originated from the ordered distribution of metal nanoparticles. Therefore, any photonic band effect can be ignored. Third, each metal nanoparticle behaves like dipoles during the whole process of excitation and relaxation [29]. Under these assumptions, classical Clausius-Mossotti formula for polarizability of small particles α

$$\alpha = 3V\frac{\varepsilon - \varepsilon_m}{\varepsilon + 2\varepsilon_m} \tag{6}$$

holds, where V is the particle volume, ε and ε_m are the permittivities of the particle and the surrounding medium, respectively (Here, $\varepsilon_m = 1$). Using the Clausius-Mossotti formula and introducing the volume fraction of the inclusions f, we can obtain Maxwell-Garnett formula

$$\frac{\varepsilon_{\text{eff}} - 1}{\varepsilon_{\text{eff}} + 2} = f\frac{\varepsilon_{\text{naanoparticle}}(R,\omega) - 1}{\varepsilon_{\text{naanoparticle}}(R,\omega) + 2} \tag{7}$$

where $\varepsilon_e ff$ is the effective dielectric function of the gold nanoparticle thin film.

The validity of our assumptions can be justified by recently available experimental conditions. First, the gold nanoparticles smaller than 10 nm show strong dipolar resonances in the quasi-static limit ($2\ R \ll \lambda$)

[25]. Second, evenly, but not lattice-like distributed gold nanoparticles can be achievable by various lithographic techniques such as block co-polymer method [29]. Therefore, effective local electric field experienced by each particle can be assumed to satisfy Lorentz cavity condition. Even though the original Maxwell-Garnett effective medium theory is valid for very small volume fraction ($f < 0.01$) [30, 31], it has been known that Maxwell-Garnett theory can successfully explain the gold nanoparticle thin film (without graphene) very well up to volume fraction $f = 0.5$ [29].

Calculating dynamic dielectric constants of composite structure requires detailed band structure calculation and exact nanoparticle configurations on the graphene. Instead, we use simpler alternative way of calculating total optical conductivity by Fresnel's approach for mixing two layer's optical properties. We can imagine a Lorentz cavity for two-dimensional spheres since the thickness of the film consisting of gold nanoparticles is much smaller than the wavelength we consider. We describe it with the two-dimensional in-plane (or surface) conductivity $\sigma^{(2D)}$ using the following two relations: The first relation is the relation between complex (effective) dielectric function and three-dimensional conductivity $\sigma^{(3D)}$, as shown in Eq. (8). The second relation connects 2D conductivity and 3D conductivity with the thickness $h = 2R$, as shown in Eq. (9).

$$\varepsilon_{eff} = 1 + i\frac{\sigma^{(3D)}}{\omega\varepsilon_0} \tag{8}$$

$$\sigma^{(2D)} = h \times \sigma^{(3D)} \tag{9}$$

Combining these relations in Eq. (8) and (9), we can obtain the two-dimensional in-plane conductivity of the gold nanoparticle thin film:

$$\sigma^{(2D)}_{\text{gold}} = 2R \times (\varepsilon_{\text{eff}} - 1)\frac{\omega\varepsilon_0}{i} \tag{10}$$

Now we assume the incident electromagnetic field is in parallel to the plane so total conductivity can be obtained by the sum of each conductivity such that:

$$\sigma_{\text{total}} \approx \sigma_{\text{graphene}} + \sigma^{(2D)}_{\text{gold}} \tag{11}$$

This assumption is based on the interlayer coupling is much smaller than the incident optical energy [32]. We note that inclined illumination on the composite would increase coupling between graphene and individual metal nanoparticles. We note that this calculation provides surprisingly good agreements with recent experimental data [13]. We also note that the addition of two optical conductivities can only be validated in the linear response regime and under the quasi-static limit.

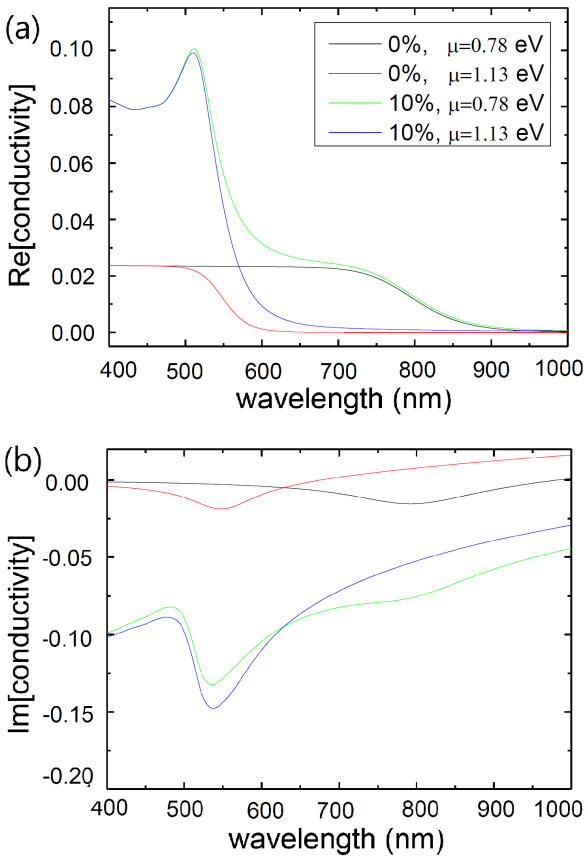

Fig. 3. (Color online) The real (a) and imaginary (b) spectra of the optical conductivity of the graphene-gold nanoparticle composite on the effect of the chemical potential change and gold nanoparticle volume fraction. We have plotted for volume fractions 0% and 10% at 373 K for two different chemical potentials 0.78 eV and 1.13 eV.

IV. THE OPTICAL CONDUCTIVITY OF THE GRAPHENE WITH AU NANOPARTICLLES AT ROOM TEMPERATURE

From now on, we assume the whole system is in thermal equilibrium to make the electronic temperature T same as the phonon temperature of the system. This can

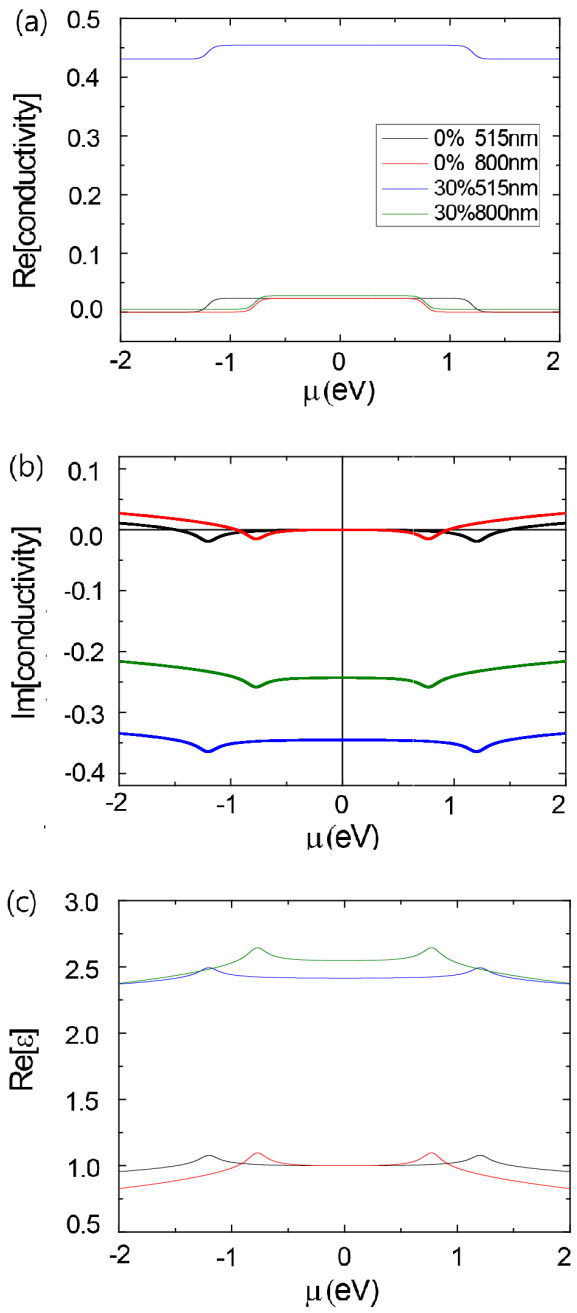

Fig. 4. (Color online) The real (a), imaginary (b) parts of the conductivities and the dielectric function (c) as a function of the chemical potential for two wavelengths at 515 nm and 800 nm. We have plotted for volume fractions 0% and 30% at 373 K. The radius of the gold particles is $\sim$ 10 nm.

describe the situation when the external light at constant intensity is incident on the graphene. Fig. 2(c) and (d) show the real and imaginary part of the conductivity as a function of the volume fractions of the gold nanoparticles at 373 K, respectively. As the volume fraction of the gold nanoparticles increases, several interesting properties in the total conductivity emerge: First, the real (imaginary) values increase (decrease) drastically for more than 1000%. Second, conductivity peaks, which give selectivity to the system, are red-shifting. Third, step-like behavior at $\hbar\omega = 2\mu$ becomes smeared out (See black line near 800 nm in the Fig. 2(c) and (d)).

It is informative to compare these radical changes in the optical conductivities with well-known chemical potential shift μ on the suspended graphene by gating electric field [33–35]. For the gated graphene, the step-like singular features in the spectra show blue-shift as chemical potential increases. If we compare optical conductivities of intrinsic graphene at 0.78 eV (black) and 1.13 eV (red), as shown in Fig. 3, about 2% of the change can be obtained in the internal between 550 $\sim$ 800 nm. However, approximately 10% of the conductivity change can be obtained with 10% volume fraction of the gold nanoparticles for spectral region 500 nm or less. (See green (10% at 0.78 eV) and blue (10% at 1.13 eV) in Fig. 3). The peak at 500 nm is originated from the surface plasmon resonance of the gold nanoparticles. We note that the plasmonic resonance originated from the gold nanoparticles and the electrostatic gating can be observed separately as slopes of the spectrum as shown in the green curve for the case of 10% at 0.78 eV.

For further study on the chemical potential dependence, we have plotted the conductivity as a function of the chemical potential for two wavelengths, as shown in Fig. 4. We find that the shape of the conductivities of the mixture does not change and the spectra merely shift in parallel. This shift is largely originated from the sum of the imaginary parts of the conductivities and has a profound meaning for optical response of the composite. If we recall the previous relation of Eq. (10) connecting the 3D dielectric constant and the 2D conductivity, *i.e.* $\varepsilon^{(3D)} = 1 + i\sigma^{(2D)}/(2R\omega\varepsilon_0)$, the increased negative imaginary value of the 2D conductivity implies decreased positive value of the dielectric constants for the mixture. Therefore, the dielectric constant mismatch between air and mixture and the total reflection would decrease. (This will be discussed in Fig. 7(b) again.) We note that, when $\hbar\omega = 2\mu$, step-function-like behavior always appears according to the pure graphene properties

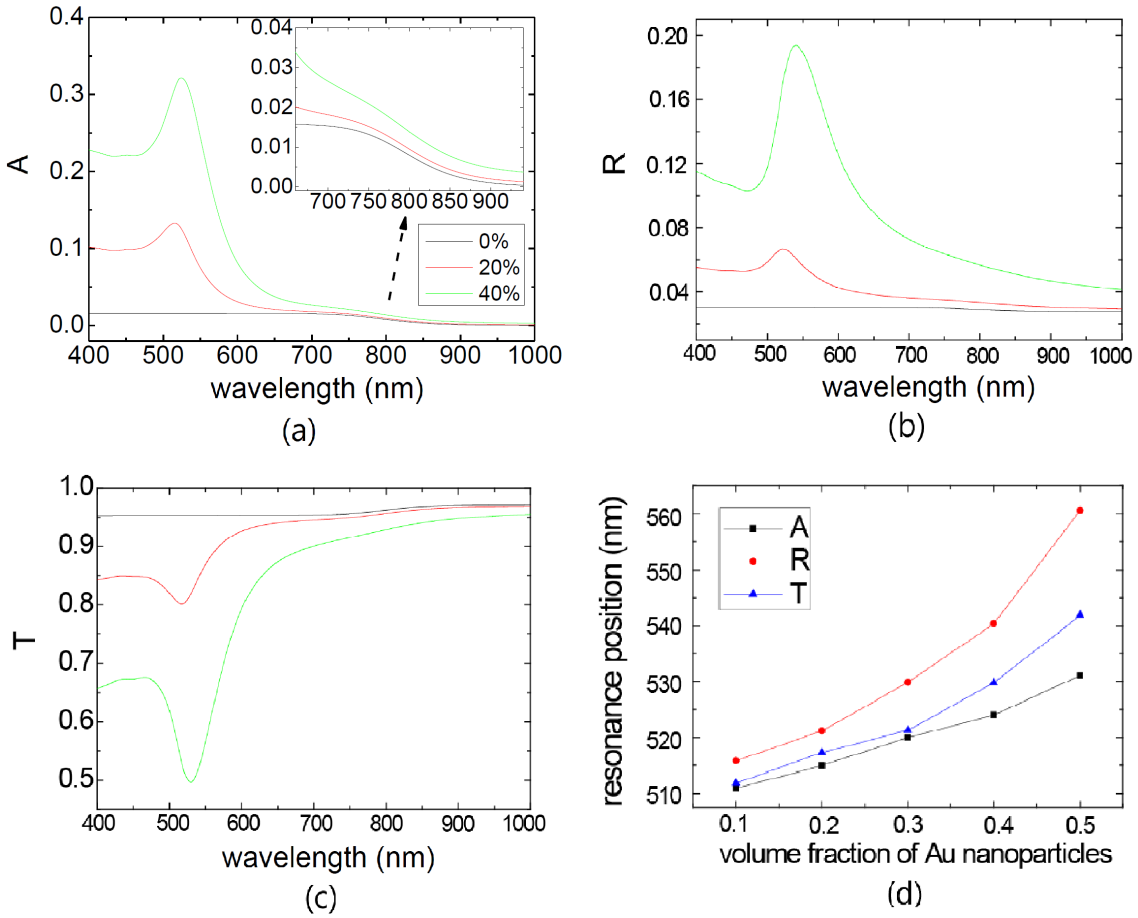

Fig. 5. (Color online) (a) Absorptance, (b) reflectance, and (c) transmittance spectra for three different volume fractions. As the volume fraction increases absorption and reflection (transmission) increase (decreases) and the peak points are red-shifted. The peak point in the absorptance spectra lies at 515 nm and 526 nm for volume fraction 20% and 40%, respectively. These absorptance spectra support the experimental data [13]. The inset shows the smeared Heaviside-step functions near the 800 nm. (d) The resonance peak positions show slight red-shifts with increased volume fraction.

except for the case when the location of the slope and the plasmonic resonance happens to coincide.

Experimentally, the chemical doping effect of the gold nanoparticles on the graphene is controversial. There are many pieces of evidence for different doping effects of the gold nanoparticles on the graphene depending on the configuration and distances [36–39]. This effect would eventually break the symmetry of the optical conductivity spectra described as a function of the chemical potential. Note that our model does neither consider the local doping effect of the gold nanoparticles nor discriminate the pure optical effects from the gold nanoparticles and the roles as local dopants. However, the local doping effect has known to show a dramatic change of the optical response of the graphene mostly by enhancing carrier concentration of the graphene [40–42]. The effect of gold nanoparticles on the graphene sheet has been interpreted as local charge reservoirs for enhancing carrier concentration of the graphene [42].

Optically, gold nanoparticles can work as local dipole antennae that efficiently capture incident electromagnetic waves and excite localized surface plasmons [13]. Even though we are not trying to clarify the role of the gold nanoparticles by discriminating doping effect versus antenna effect, we emphasize that altered optical conductivity and the doping effect share common background on the total response of the composite: plasma frequency ω_p. The plasma frequency of the whole system may share information of the Drude-like optical response as well as the information of free carrier density of the composite. Clarification of the role of gold nanoparticles is still an open question.

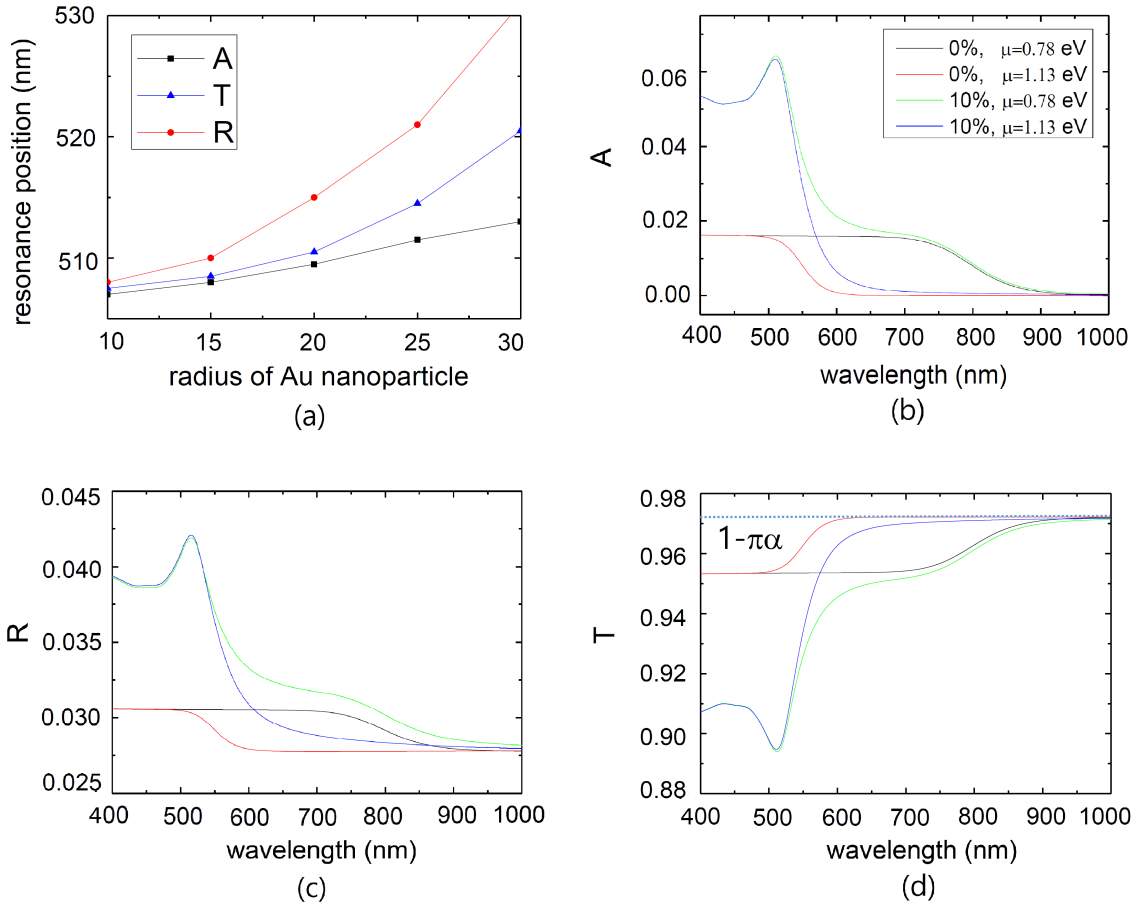

Fig. 6. (Color online) Absorptance, transmittance, and reflectance peak positions are shown as a function of the radius of gold nanoparticles at 373 K. The chemical potential is set to 0.775 eV. The absorptance (b), the reflectance (c), and the transmittance (d) spectra of the graphene + gold nanoparticle composite system. As the chemical potential increases, the step-like behaviors are blue-shifted. Note that the reflectance spectra are affected by both real and imaginary part of the conductivity whereas the absorptance spectra show feature originated only from the real part of the conductivity.

V. TRANSMITTANCE, REFLECTANCE, AND ABSORPTANCE OF THE EFFECTIVE THIN LAYER

In this section, we study the physically observable properties: Transmittance, reflectance, and absorptance under normal incident light. The considered system is same as the previous composite material made of air, gold nanoparticles, graphene, and glass substrate (as shown in Fig. 2). The refractive indices of air and SiO^2 are chosen as $n_1 = 1$ and $n_2 = 1.4$. Solving the Maxwell equations with an appropriate boundary conditions for normal incident light gives the transmittance, reflectance, and absorptance [23]:

$$T = \frac{n_2}{n_1}\left|\frac{2n_1}{n_1 + n_2 + \frac{\sigma(\omega)}{c\varepsilon_0}}\right|^2 \approx \frac{1.4}{1.2^2}\left(1 - \frac{\mathrm{Re}[\sigma(\omega)]}{1.2c\varepsilon_0}\right), \tag{12}$$

$$R = \left|\frac{n_2 - n_1 + \frac{\sigma(\omega)}{c\varepsilon_0}}{n_2 + n_1 + \frac{\sigma(\omega)}{c\varepsilon_0}}\right|^2 = \left|\frac{0.4 + \frac{\sigma(\omega)}{c\varepsilon_0}}{2.4 + \frac{\sigma(\omega)}{c\varepsilon_0}}\right|^2, \tag{13}$$

$$A = 1 - T - R, \tag{14}$$

where $\sigma(\omega)$ is the total surface conductivity of the graphene with gold nanoparticles. When the $\frac{\sigma(\omega)}{c\varepsilon_0}$ is small we can obtain an approximate expression for T as

$$T \approx \frac{1.4}{1.2^2}\left(1 - \frac{\mathrm{Re}[\sigma(\omega)]}{1.2c\varepsilon_0}\right).$$

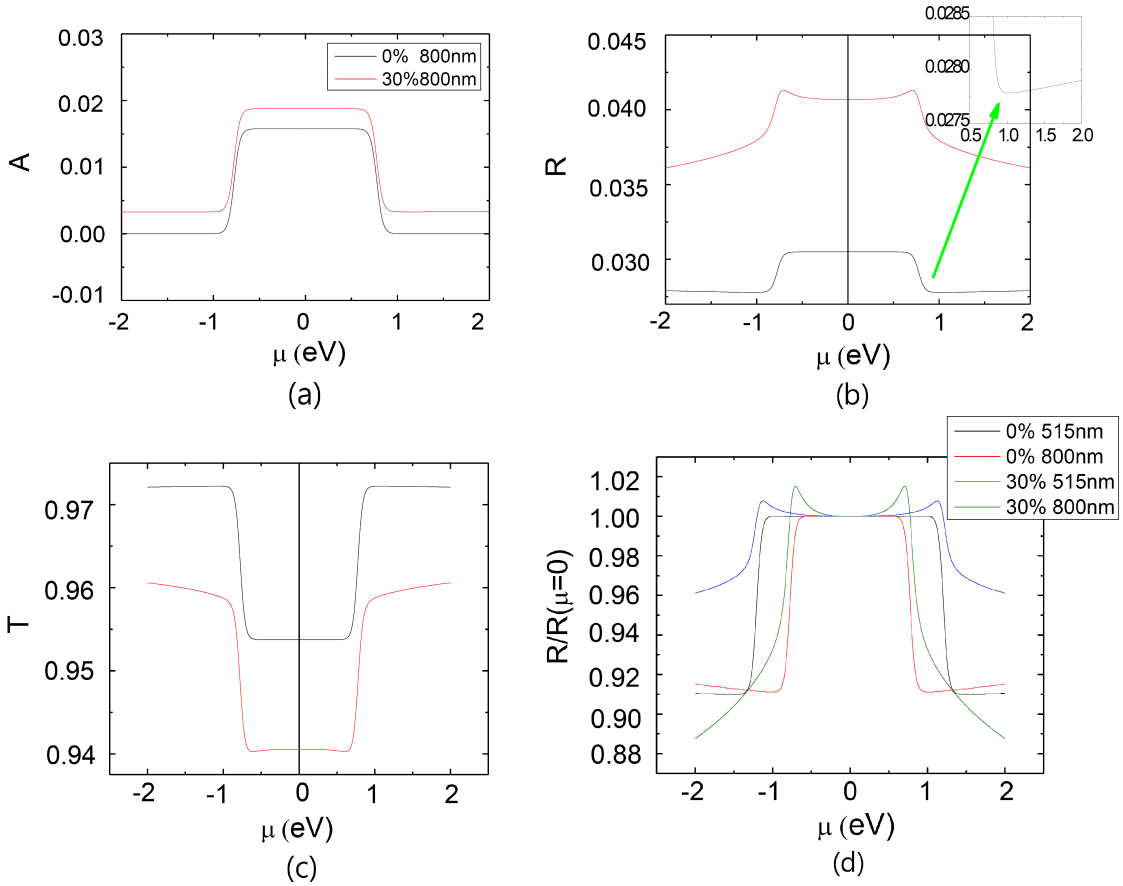

Fig. 7. (Color online) (a) The absorptance spectra as a function of the chemical potential. A step-like behavior can be seen. (b) The reflectance spectra as a function of the chemical potential. When the chemical potential is larger than 1 eV, the reflectance of 30% mixture shows decreasing behavior whereas the pure graphene shows increasing behaviors (See the inset). (c) The transmittance spectra as a function of the chemical potential. (d) The ratio of reflectance $R(\mu)/R(\mu = 0)$ as a function of the chemical potential for two different volume fraction and at two different wavelengths. At 800 nm, more than 9% reflectance change can be obtained from the 30% composite by tuning the chemical potential $\sim$ 320 meV.

We plot absorptance, transmittance and reflectance spectra for various volume fractions as shown in Fig. 5. The absorptance, transmittance and reflectance spectra of the pure graphene is nearly constant but only change near $\hbar\omega = 2\mu$ (See black lines in the Fig. 5), which is a well-known optical property of intrinsic graphene. However, if we put the gold thin film on the graphene sheet, there are enhancement and resonance peak points in the absorptance, reflectance and transmittance spectra due to the localized surface plasmon resonance effect of the gold nanoparticles as shown in the red and green lines in Fig. 5. We observe that the increased volume fraction leads to the red-shift of the resonance peak. The enhanced absorption can make the composite useful as a photodetector [12,13,43].

Let us consider the effect of the size of the gold nanoparticles. For simplicity, we assume that the gold nanoparticles are spread randomly, but uniformly on graphene with average lattice spacing $a = 80$ nm. Then, the volume fraction is given by

$$f = \frac{4}{3}\pi R^3/(a^2 2R) \propto R^2. \qquad (15)$$

Fig. 6(a) shows the absorption resonance position for various radii of gold nanoparticles. As expected, the peak positions show red-shifts with increased radius of the gold nanoparticles. These shifts are attributed to the decreased surface plasmon resonance energy of individual nanoparticles.

Now let us look at the optical properties of the mixture as a function of the chemical potential. Fig. 6 shows the

absorptance (b), reflectance (c), and transmittance (d) spectra when the chemical potential is set either at 0.78 eV or 1.13 eV, respectively. The absorptance spectra resemble the real part of the optical conductivity as shown in Fig. 3(a). However, reflectance spectra are affected by both the real and the imaginary values of the conductivity (See Eq. (13) and Fig. 6(c)). From the transmittance spectra, the low energy transmittance asymptotically approaches

$$T \approx 1 - \pi\alpha, \tag{16}$$

where α is the fine structure constant [8, 44]. This transparency condition is a unique feature from two-dimensional materials, and our composite material shows similar characteristics. However, it should be noted that the absorptance of the composite is not $\pi\alpha$ anymore like the case of pure graphene. We obtain a non-negligible reflection from the composite as shown in Fig. 6(c). It is surprising that the same transparency condition (16) could be obtained after considering non-negligible absorption and reflection from our composite. The origin of the transparency of 2-dimensional materials is currently under debate [44].

To figure out the effect of chemical potential and the corresponding tunability, we have plotted absorptance, reflectance, and transmittance spectra as shown in Fig. 7. The change of the reflectance with respect to the chemical potential is much larger than that of the pure graphene (See Fig. 7(b)), which allows the combination of graphene and gold nanoparticle more useful for a tunable device. To compare the change of the reflection, we have plotted the ratio $R(\mu)/R(\mu = 0)$ with respect to the chemical potential as shown in Fig. 7(d). For 30% volume fraction, the normalized reflectance at 800 nm increases up to 0.71 eV of the chemical potential. The normalized reflectance suddenly drops more than 9% with ∼320 meV change of the chemical potential. The ratio for the pure graphene increases slightly for $\mu > 1.5\ eV$.

The step-like behaviors near $\hbar\omega = 2\mu$ in the previous figures (For example, see green lines in Fig. 6), comes from the smeared step-function of the real part of the conductivity for the pristine graphene. At low temperature, those step-behaviors can appear clearly as shown in Fig. 8. With gold nanoparticles, though, this feature would be submerged into the predominant plasmon resonance peak. With 10% of volume fraction, a small change of the slope might be observable at 10 K. However, the optical properties of the composite at low temperature are essentially same [24,45].

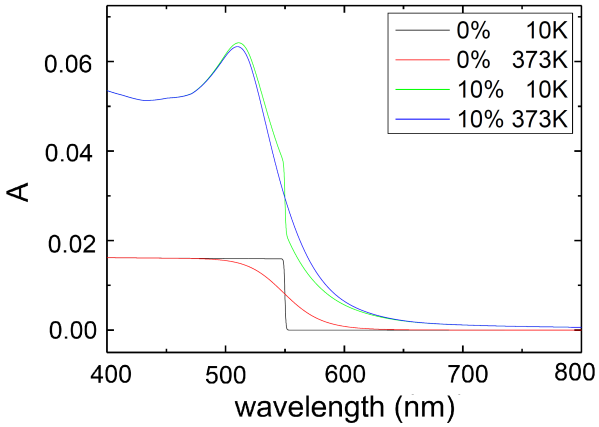

Fig. 8. (Color online) Absorptance spectra at two different temperatures 10 K and 373 K. The chemical potential is set to 1.13 eV. As temperature goes down, the step-like behaviors may be seen from non-zero volume fraction samples.

VI. CONCLUSION

In this paper, we used Maxwell-Garnet effective medium theory to investigate the optical response of the gold nanoparticles on a single graphene sheet on a glass substrate. We quantitatively estimated the effects of the filling of gold nanoparticles, the chemical potential, and temperature on absorptance, reflectance, and transmittance. The effect of a mixture of the gold nanoparticles and graphene can be understood as the results of propagating electromagnetic waves along the mixture with localized dipolar surface plasmon resonance of each metal particle. The reflectance of the graphene with gold nanoparticles shows changes ∼9% under the chemical potential, which allows feasible reflective photonic modulator applications. Our approach can apply to other composite systems made of graphene with other metallic nanoparticles.

ACKNOWLEDGEMENTS

This research was supported by newly appointed professor research fund of Hanbat National University in 2016.

REFERENCES

[1] A. K. Geim and K. S. Novoselov, Nat. Mater. **6**, 183 (2007).
[2] K. S. Novoselov, A. K. Geim, S. V. Morozov, D. Jiang and Y. Zhang *et al.*, Science **306**, 666 (2004).
[3] A. H. C. Neto, F. Guinea, N. M. R. Peres, K. S. Novoselov and A. K. Geim, Rev. Mod. Phys. **81**, 109 (2009).
[4] F. Schwierz, Nat. Nanotechnol. **5**, 487 (2010).
[5] F. Bonaccorso, Z. Sun, T. Hasan and A. C. Ferrari, Nat. Photonics **4**, 611 (2010).
[6] P. Avouris, Nano Lett. **10**, 4285 (2010).
[7] C. Lee, X. Wei, J. W. Kysar and J. Hone, Science **321**, 385 (2008).
[8] R. R. Nair, P. Blake, A. N. Grigorenko, K. S. Novoselov and T. J. Booth *et al.*, Science **320**, 1308 (2008).
[9] K. I. Bolotin, K. J. Sikes, Z. Jiang, M. Klima and G. Fudenberg *et al.*, Solid State Commun. **146**, 351 (2008).
[10] F. Xia, T. Mueller, Y. Lin, A. Valdes-Garcia and P. Avouris, Nat. Nanotechnol. **4**, 839 (2009).
[11] T. Mueller, F. Xia and P. Avouris, Nat. Photonics **4**, 297 (2010).
[12] Y. Liu, R. Cheng, L. Liao, H. Zhou and J. Bai *et al.*, Nat. Commun. **2**, 579 (2011).
[13] U. J. Kim, S. Yoo, Y. Park, M. Shin and J. Kim *et al.*, ACS Photonics **2**, 506 (2015).
[14] I. Gierz, C. Riedl, U. Starke, C. R. Ast and K. Kern, Nano Lett. **8**, 4603 (2008).
[15] K. T. Chan, J. B. Neaton and M. L. Cohen, Phys. Rev. B **77**, 235430 (2008).
[16] R. Muszynski, B. Seger and P. V. Kamat, J. Phys. Chem. C **112**, 5263 (2008).
[17] H. M. A. Hassan, V. Abdelsayed, A. E. R. S. Khder, K. M. AbouZeid and J. Terner *et al.*, J. Mater. Chem. **19**, 3832 (2009).
[18] J. Li and C. Liu, Eur. J. Inorg. Chem. **2010**, 1244 (2010).
[19] N. M. R. Peres, Rev. Mod. Phys. **82**, 2673 (2010).
[20] V. P. Gusynin and S. G. Sharapov, Phys. Rev. B **73**, 245411 (2006).
[21] S. A. Mikhailov and K. Ziegler, Phys. Rev. Lett. **99**, 016803 (2007).
[22] L. A. Falkovsky and S. S. Pershoguba, Phys. Rev. B **76**, 153410 (2007).
[23] T. Stauber, N. M. R. Peres and A. K. Geim, Phys. Rev. B **78**, 085432 (2008).
[24] U. Kreibig, J. Phys. F: Met. Phys. **4**, 999 (1974).
[25] R. D. Averitt, D. Sarkar and N. J. Halas, Phys. Rev. Lett. **78**, 4217 (1997).
[26] R. D. Averitt, S. L. Westcott and N. J. Halas, J. Opt. Soc. Am. B **16**, 1824 (1999).
[27] S. Link and M. A. El-Sayed, J. Phys. Chem. B **103**, 4212 (1999).
[28] N. W. Ashcroft and N. D. Mermin, *Solid State Physics* (Harcourt College Publishers, New York, London, 1976).
[29] T. Ung, L. M. Liz-Marzán and P. Mulvaney, Colloids Surfaces A Physicochem. Eng. Asp. **202**, 119 (2002).
[30] G. A. Niklasson, C. G. Granqvist and O. Hunderi, Appl. Opt. **20**, 26 (1981).
[31] V. Myroshnychenko, E. Carbó-Argibay, I. Pastoriza-Santos, J. Pérez-Juste and L. M. Liz-Marzán *et al.*, Adv. Mater. **20**, 4288 (2008).
[32] K. F. Mak, M. Y. Sfeir, J. A. Misewich and T. F. Heinz, Proc. Natl. Acad. Sci. **107**, 14999 (2010).
[33] F. Wang, Y. Zhang, C. Tian, C. Girit and A. Zettl *et al.*, Science **320**, 206 (2008).
[34] C.-F. Chen, C.-H. Park, B. W. Boudouris, J. Horng and B. Geng *et al.*, Nature **471**, 617 (2011).
[35] D. K. Efetov and P. Kim, Phys. Rev. Lett. **105**, 256805 (2010).
[36] K. K. Kim, A. Reina, Y. Shi, H. Park and L. J. Li *et al.*, Nanotechnology **21**, 285205 (2010).
[37] K. S. Subrahmanyam, A. K. Manna, S. K. Pati and C. N. R. Rao, Chem. Phys. Lett. **497**, 70 (2010).
[38] S. Huh, J. Park, K. S. Kim, B. H. Hong and S. Bin Kim, ACS Nano **5**, 3639 (2011).
[39] Z. Osváth, A. Deátk, K. Kertétsz, G. Molnátr and G. Vétrtesy *et al.*, Nanoscale **7**, 5503 (2015).

[40] Z. Fang, Y. Wang, Z. Liu, A. Schlather and P. M. Ajayan *et al.*, ACS Nano **6**, 10222 (2012).

[41] Z. Fang, S. Thongrattanasiri, A. Schlather, Z. Liu and L. Ma *et al.*, ACS Nano **7**, 2388 (2013).

[42] Y. Shi, K. K. Kim, A. Reina, M. Hofmann and L. J. Li *et al.*, ACS Nano **4**, 2689 (2010).

[43] M. E. Ayhan, G. Kalita, M. Kondo and M. Tanemura, RSC Adv. **4**, 26866 (2014).

[44] D. J. Merthe and V. V. Kresin, Phys. Rev. B **94**, 205439 (2016).

[45] U. Kreibig, J. Phys. Colloq. **38**, C2 (1977).